Journal of *Marine Science and Engineering*

MDPI

Article

A Complete Coverage Path Planning Approach for an Autonomous Underwater Helicopter in Unknown Environment Based on VFH+ Algorithm

Congcong Ma [1], Hongyu Zou [1] and Xinyu An [2,*]

[1] Marine Science and Technology College, Zhejiang Ocean University, Zhoushan 316022, China; macongcong@zjou.edu.cn (C.M.); zouhongyu@zjou.edu.cn (H.Z.)
[2] Ocean College, Zhejiang University, Zhoushan 316021, China
* Correspondence: anxinyu@zju.edu.cn

Abstract: An Autonomous Underwater Helicopter (AUH) is a disk-shaped, multi-propelled Autonomous Underwater Vehicle (AUV), which is intended to work autonomously in underwater environments. The near-bottom area sweep in unknown environments is a typical application scenario, in which the complete coverage path planning (CCPP) is essential for AUH. A complete coverage path planning approach for AUH with a single beam echo sounder, including the initial path planning and online local collision avoidance strategy, is proposed. First, the initial path is planned using boustrophedon motion. Based on its mobility, a multi-dimensional obstacle sensing method is designed with a single beam range sonar mounted on the AUH. The VFH+ algorithm is configured for the heading decision-making procedure before encountering obstacles, based on their range information at a fixed position. The online local obstacle avoidance procedure is simulated and analyzed with variations of the desired heading direction and corresponding polar histograms. Finally, several simulation cases are set up, simulated and compared by analyzing the heading decision in front of different obstacle situations. The simulation results demonstrate the feasibility of the complete coverage path planning approach proposed, which proves that AUH completing a full coverage area sweep in unknown environments with a single beam sonar is viable.

Keywords: complete coverage path planning (CCPP); Autonomous Underwater Helicopter (AUH); online obstacle avoidance; single beam sensor-based planning; VFH+ algorithm

Citation: Ma, C.; Zou H.; An, X. A Complete Coverage Path Planning Approach for an Autonomous Underwater Helicopter in Unknown Environment Based on VFH+ Algorithm. *J. Mar. Sci. Eng.* **2024**, *12*, 412. https://doi.org/10.3390/jmse12030412

Academic Editor: Rafael Morales

Received: 5 January 2024
Revised: 16 February 2024
Accepted: 22 February 2024
Published: 26 February 2024

1. Introduction

An Autonomous Underwater Helicopter (AUH) is an innovative, disk-shaped, multi-propelled Autonomous Underwater Vehicle (AUV). It was conceptually proposed by Ying Chen in Zhejiang University in 2017 and was invented and developed for near sea bottom operations [1]. AUH can take off/land vertically and hover at a fixed location in underwater environments like a "helicopter" in the water, and this is the origin of its name. A series of AUHs from kilogram-class education models to hundred-kilogram-class models. Great and special-purpose models have been designed and fabricated. The pool test proves their overwhelming horizontal and vertical maneuverability over the traditional torpedo-shaped AUV. AUH typically has the disk-shape design and multiple horizontal/vertical propellers layout, which gives it an advantage in full-direction turnaround, turning radius, spot hovering, and near-bottom sailing over traditional slender AUV. This design provides multiple degrees of freedom of motion, which is extremely beneficial for AUH's near-bottom operation.

Various works have been conducted related to mechanical design [2], motion stability analysis [3,4], streamlined contour optimization [5,6], motion controller design [7,8] and so on. However, there are comparatively few studies focused on AUH's operation control and autonomous path planning. Survey and observation in an interesting sea area with some

acoustic and optical equipment is one of its typical application scenarios. In AUH's near-bottom survey or observation missions, it is necessary for AUH to sweep a certain seafloor area autonomously, even though the underwater environment is unfamiliar or unknown in advance. In this circumstance, the obstacle avoidance and autonomous Complete Coverage Path Planning (CCPP) are essential functions for AUH to implement its assigned tasks. A hypothetical working scenario of AUH is shown in Figure 1.

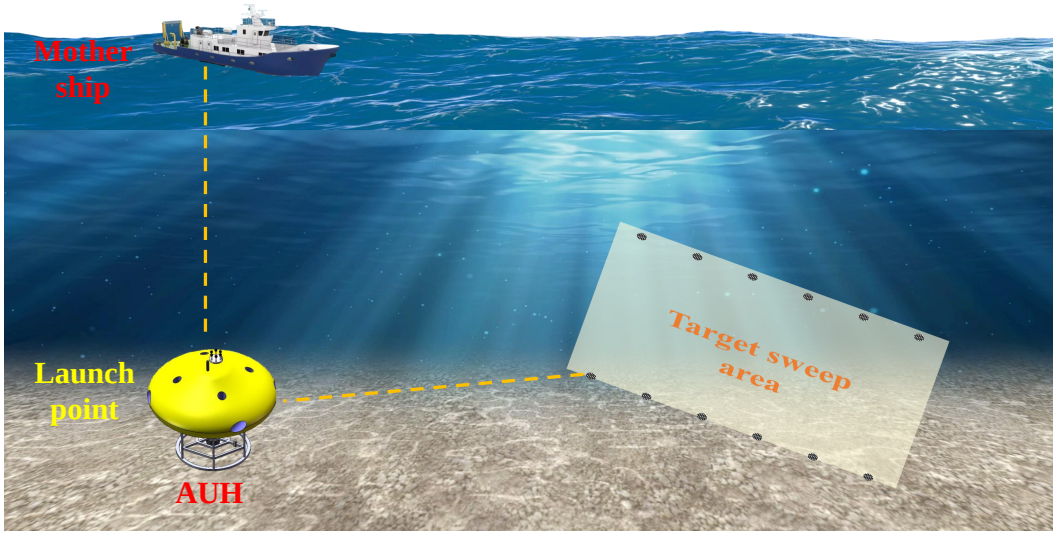

Figure 1. A hypothetical working scenario of AUH operating near-bottom including point-to-point cruising and task-based area sweeping.

Complete Coverage Path Planning algorithms have been extensively used in practical applications such as cleaning of sweeping robots, mine sweeping, surveillance [9], harvesting fruits in agriculture [10], and underwater operations [11]. CCPP algorithms are characterized as classical, heuristic, and, most recently, deep learning methods. For the complete coverage path planning, it is usually supposed that the environment is closed or the operation area is restricted and the operation boundary can be given at the beginning or detected by robots. The whole target area is decomposed into several subdomains and the robot sweeps all subdomain to cover the entire target area. The environment decomposition technique and backtracking mechanism are two important criteria considered while performing traditional CCPP algorithms [12]. Subsequently, various types of obstacle avoidance algorithms are developed to circumvent detected obstacles, of which artificial potential field, Vector Field Histogram (VFH), its variants (VFH+, VFH*, etc.), and A* are widely used. Cell-based decomposition, especially the exact cell-based decomposition, which is simple and straightforward to implement, is the most commonly used approach for environment decomposition, especially in outdoor atmospheres [13]. In most cases, some forms of decomposition like Boustrophedon [14], Semi-boustrophedon [15], Morse [16], or Line-sweep decomposition [17], are used to partition the free space into a set of non-overlapping cells. An improved VFH algorithm with Apollonius circle and information sharing strategy is also effective in real-time obstacle avoidance with the goal of guiding Unmanned Aerial Vehicle (UAV) swarms in an unknown complicated environment [18]. The VFH+-based shared control method for remotely controlled mobile robots was evaluated in a navigation task in a simulated disaster site and it provided a significant improvement in terms of safety and task completion time compared to teleoperation [19]. Boustrophedon motions and the A* search algorithm (BA*) was used by an autonomous cleaning robot to solve the online complete coverage task in an unknown workspace [20]. A complete coverage path planning model was trained using deep reinforcement learning (RL) for the tetromino-based reconfigurable robot in autonomous complete area coverage tasks such as floor cleaning, building inspection, and maintenance, surface painting [21]. An approach solely relying on a single monocular camera with deep reinforcement learning

(DRL) is investigated for a robot to avoid obstacles in simple 3D environments, and the simulation result indicates a promising direction to continue research on DRL for mapless navigation [22]. These decomposition methods and obstacle avoidance algorithms developed and adopted for various robots are well behaved and support them in accomplishing predefined tasks. These approaches are quite instructive for AUH's autonomous CCPP missions. Based on previous research, the effective combination of the obstacle avoidance strategy with AUH's superior maneuverability is well worth studying.

Despite various developed CCPP algorithms, the special operation mode makes them not perfectly appropriate for AUH's navigation control strategy. The existence of an obstacle is perceived by the distance information given by a horizontally mounted single beam range sonar/echo sounder (as can be seen in Figure 2), and it obviously distinguishes from other robots, on which LiDAR [23], infrared distance sensor, ultrasonic sensor [24], millimeter wave radar [25], camera, and multi-beam sonar [26], etc. are frequently used. However, the detection distance is generally much larger than AUH's geometric dimensions, which makes it adequate to take more attempts to get around obstacles. Besides, the echo sounder only acquire a distance information in one direction on one measurement, and it is not sufficient for AUH to take collision avoidance action. Hence, special treatment is necessary to obtain enough obstacle information to serve as the input of the collision avoidance algorithm.

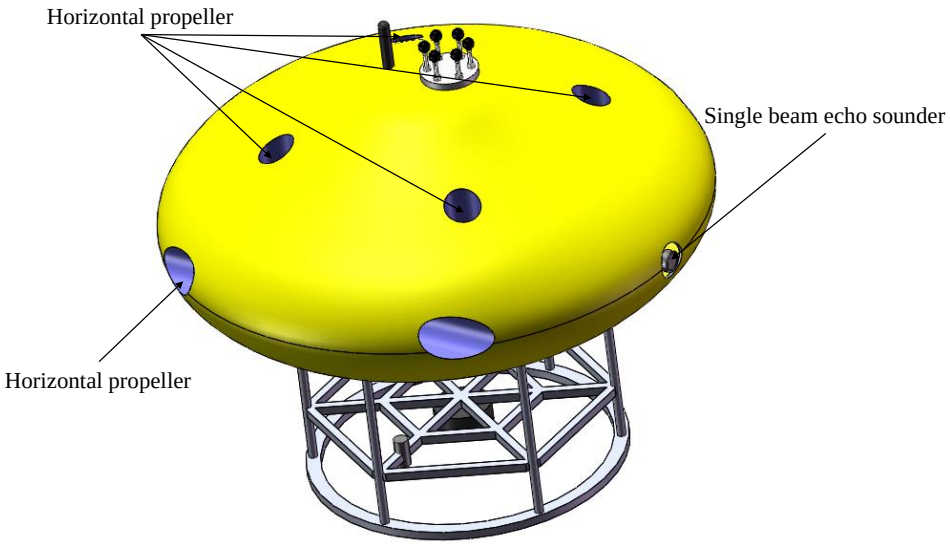

Figure 2. A typical layout design of AUH with multiple propellers and a single-beam echo sounder.

Taking advantage of AUH's maneuverability, the main issue of this paper is to propose an effective approach to fulfill AUH's CCPP using a single-beam sensor rather than the common expensive multi-beam obstacle avoidance sonar. Therefore, making use of AUH's horizontal mobility, a multiple obstacle detection strategy using a single beam sensor is introduced to accomplish a similar function to that of the multibeam device. Then, combined with the initial path planning and local obstacle avoidance algorithm, a CCPP approach suitable for AUH is fulfilled.

In this paper, a complete coverage path planning approach for AUH, which is a new type of AUV with high mobility, is proposed, including the initial path planning and online local collision avoidance strategy. This paper is organized as follows. First, the initial path is planned using boustrophedon motion. Based on its mobility, a multi-dimensional obstacle sensing method is designed with a single beam echo sounder mounted on AUH. The VFH+ algorithm is configured for the heading decision-making procedure based on range information from obstacles at a fixed position. The online local obstacle avoidance procedure is simulated and analyzed with variations of the heading direction and corresponding polar

histograms. Finally, several simulation cases are set up, simulated and compared to verify the feasibility of the proposed complete coverage path planning approach.

2. Design of CCPP Approach for AUH

The entire of CCPP approach for AUH includes the initial path planning, the obstacle perception and the local collision avoidance. These three parts are designed specially for AUH working in underwater environments and are detailed in the following subsections.

2.1. Initial Path Planning with Boustrophedon Motion

The complete coverage path planning is updated based on an initial boustrophedon motion (BM) of the whole operation area. For the complete coverage path planning problem, whether prior environment information is available, an initial planned route is needed for a robot to run. The boustrophedon cellular decomposition (BCD) is exercised by most planners to design the initial path and partition the robot's free working space into a set of non-overlapping cells. Each one of these non intersecting cells can be covered by the robot with back-and-forth boustrophedic motions. During the robot working period, the complete coverage of an environment is completed once each cell is reached. The boustrophedon motion in the robot's working environment for the preliminary path planning is shown in Figure 3.

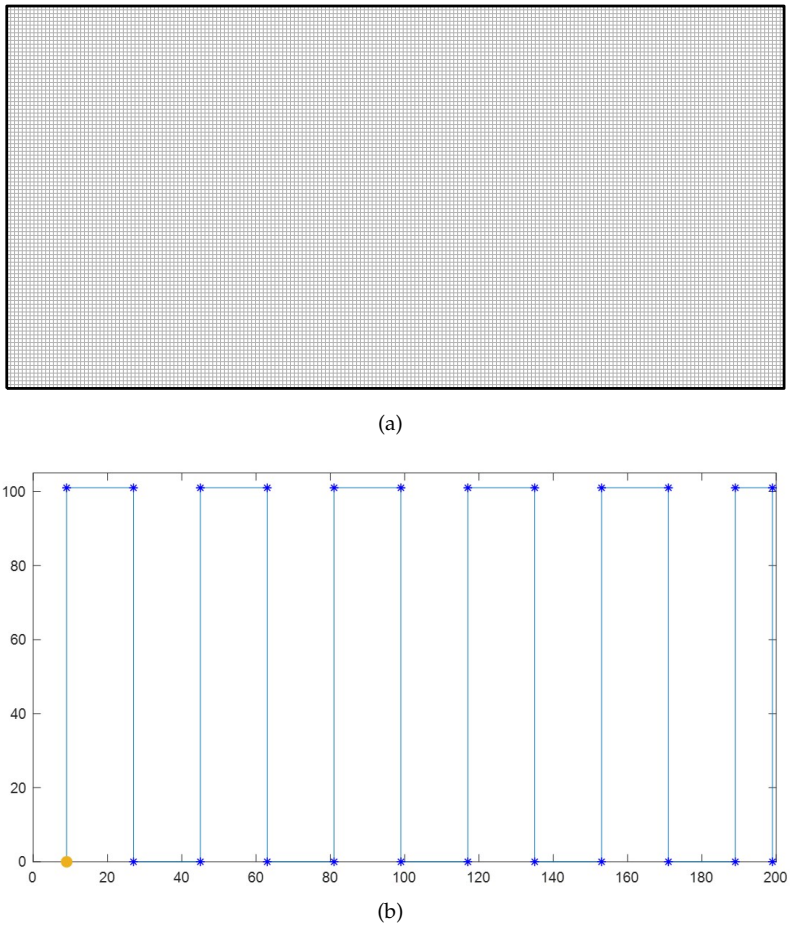

Figure 3. Boustrophedon motion path and key points for the initial complete coverage path planning. (**a**) The rasterized map of whole working area; (**b**) BM path and key points.

As shown in Figure 3a, the whole working area is rasterized, and AUH is set to work step by step in the grid map along the planned path. The entire map is preliminarily covered by the path designed by boustrophedon motion. The initial BM path and corresponding

key waypoints are illustrated in Figure 3b. The robot's transverse span is a fundamental parameter to design the boustrophedic path, which typically depends on a detect sensor's swath width.

Theoretically, a robot can implement a complete coverage of the working space by running along the initial boustrophedic path. However, the presence of obstacles is inevitable in most scenarios. Therefore, the specified obstacle detection strategy and an obstacle avoidance algorithm is necessary as well to solve the CCPP problem, especially in an unfamiliar environment. The corresponding content adopted by an AUH in this paper is discussed in the following subsection.

2.2. VFH+ Algorithm for Local Obstacle Avoidance

The VFH+ algorithm is improved from the VFH algorithm, solving its inherit problems such as ignoring the robot's size and the possible oscillation of the desired heading before obstacles. In the VFH algorithm, there are many parameters to be set and adjusted. The VFH+ algorithm can offer better results in smoother robot trajectories and greater reliability [27].

In the VFH+ algorithm, the size of robots and its detection range is considered, thus obstacle cells are enlarged by a radius:

$$r_{r+s} = r_r + d_s,$$

where r_r is the robot radius and d_s is the minimum distance that the robot needs to switch into the obstacle avoidance process. Then the robot can be considered as a point-like vehicle. The VFH+ algorithm adopts a four-stage data reduction process in order to decide the new direction of motion. In the first stage, the primary polar histogram at the robot's current point is established, which is similar to the VFH algorithm. The vector direction $\beta_{i,j}$ is calculated as follows:

$$\beta_{i,j} = \arctan(\frac{y_j - y_0}{x_i - x_0}) \tag{1}$$

where, (x_0, y_0) is the current coordinates of the robot center, and (x_i, y_j) is the coordinates of active cell $C_{i,j}$. The vector magnitude $m_{i,j}$ for an active cell $C_{i,j}$ is given by

$$m_{i,j} = c_{i,j}^2(a - bd_{i,j}^2) \tag{2}$$

where, $c_{i,j}$ is the certainty value of active cell $C_{i,j}$, $d_{i,j}$ is the distance from active cell $C_{i,j}$ to the robot center. The parameters a and b are chosen according to $a - b(\frac{w_s-1}{2})^2 = 1$. The primary polar histogram H^P has an angular resolution of α, and $s = 360^\circ/\alpha$ is an integer. In this paper, α is determined by AUH's angular turning step and is set to 1°s. Each angular sector k corresponds to a discrete angle $\varphi = k \cdot \alpha$. Thus, the primary polar histogram is built and the procedure is identical to that of the VFH algorithm.

Taking into the radius r_{r+s}, the enlargement angle $\gamma_{i.j}$ is defined by

$$\gamma_{i,j} = \arcsin(\frac{r_{r+s}}{d_{i,j}}) \tag{3}$$

For each sector, the polar obstacle density is calculated by

$$H_k^P = \sum(d_{i,j} \cdot h'_{i,j}) \tag{4}$$

where, $h'_{i,j} = 1$, if $k \cdot \alpha \in [\beta_{i,j} - \gamma_{i,j}, \beta_{i,j} + \gamma_{i,j}]$ and $h'_{i,j} = 0$, otherwise.

In the second stage, in order to eliminate the robot's oscillation between a narrow opening and other openings, two thresholds τ_{high} and τ_{low} are adopted to build a binary polar histogram H^B based on the previous primary polar histogram H^P. The sectors of H^B are either free (0) or blocked (1). At time n, the binary polar histogram is updated according to

$$\begin{aligned} H^B_{k,n} &= 1 && \text{if } H^P_{k,n} > \tau_{high} \\ H^B_{k,n} &= 0 && \text{if } H^P_{k,n} > \tau_{low} \\ H^B_{k,n} &= H^B_{k,n-1} && \text{otherwise} \end{aligned}$$

In the third stage, the robots's trajectory is assumed based on circular arcs (constant curvature curves) and straight lines. The radii for both sides are defined as $r_r = 1/\kappa_r$ and $r_l = 1/\kappa_l$, where κ is the curvature of a curve. Thus, additional blocked sectors are determined because of the robot trajectory based on following conditions:

$$\begin{aligned} d_r^2 &< (r_r + r_{r+s})^2 && \beta_{i,j} \in [\theta, \varphi_r] \\ d_l^2 &< (r_l + r_{r+s})^2 && \beta_{i,j} \in [\varphi_l, \theta] \end{aligned}$$

where, d_r and d_l are the distances from an active cell $C_{i,j}$ to the right and left trajectory centers.

With φ_l and φ_r, the masked polar histogram is built:

$$\begin{aligned} H^m_k &= 0 && \text{if } H^B_k = 0 \; and \; (k \cdot \alpha) \in [\theta, \theta] \bigcap [\theta, \varphi_r] \\ H^m_k &= 1 && \text{otherwise} \end{aligned}$$

If all sectors are blocked, the robot would have to determine a set of new values (φ_l, φ_r) based on slower speed.

In the fourth stage, firstly, candidate directions are listed from the wide and narrow openings in the masked polar histogram. Then, a cost function is defined so that the robot selects the most appropriate candidate direction as its new direction of motion φ_d. The cost function g, expressed as a function of a candidate direction c, can have the following form:

$$g(c) = \mu_1 \cdot \Delta(c, k_l) + \mu_2 \cdot \Delta(c, \frac{\theta_n}{\alpha}) + \mu_3 \cdot \Delta(c, k_{d,n-1}) \tag{5}$$

The three terms in cost function $g(c)$ correspond to the costs associated with the difference of a candidate direction and the target direction, the robot's current wheel orientation, and the previously selected direction of motion, separately. The relationship of three parameters μ_1, μ_2 and μ_3 guarantee which type of trajectory the robot prefers. For a goal-oriented mobile robot, a good set of parameters is $\mu_1 = 5$, $\mu_2 = 2$ and $\mu_3 = 2$. Other terms can also be added to the cost function to implement more subtle behavior at certain positions.

2.3. Obstacle Detection Strategy of AUH

The disk-shape design and multiple propellers layout provide an advantage in high mobility, such as turning at the original point. Thus, AUH can carry out obstacle distance detection many times at a point with a single-beam sonar, which is similar to the function of an expensive multi-beam sonar or LiDAR. In a realistic scenario, AUH conducts the obstacle detection in such a mechanism. AUH moves forward and conducts obstacle detection simultaneously. When AUH does not detect an obstacle in its current heading direction at its present position, it keeps moving on without turning. When the AUH detects an obstacle, it initially slows down, as it only has distance information in one direction. Then it turns left and right at a certain angle step continuously and takes an obstacle distance measurement at each angle direction. Thus, a series of obstacle distance information is available at its current position. The obstacle avoidance is one of AUH's sensor-based motion, which is based on AUH's superior mobility. The obstacle detection strategy diagram is shown in Figure 4.

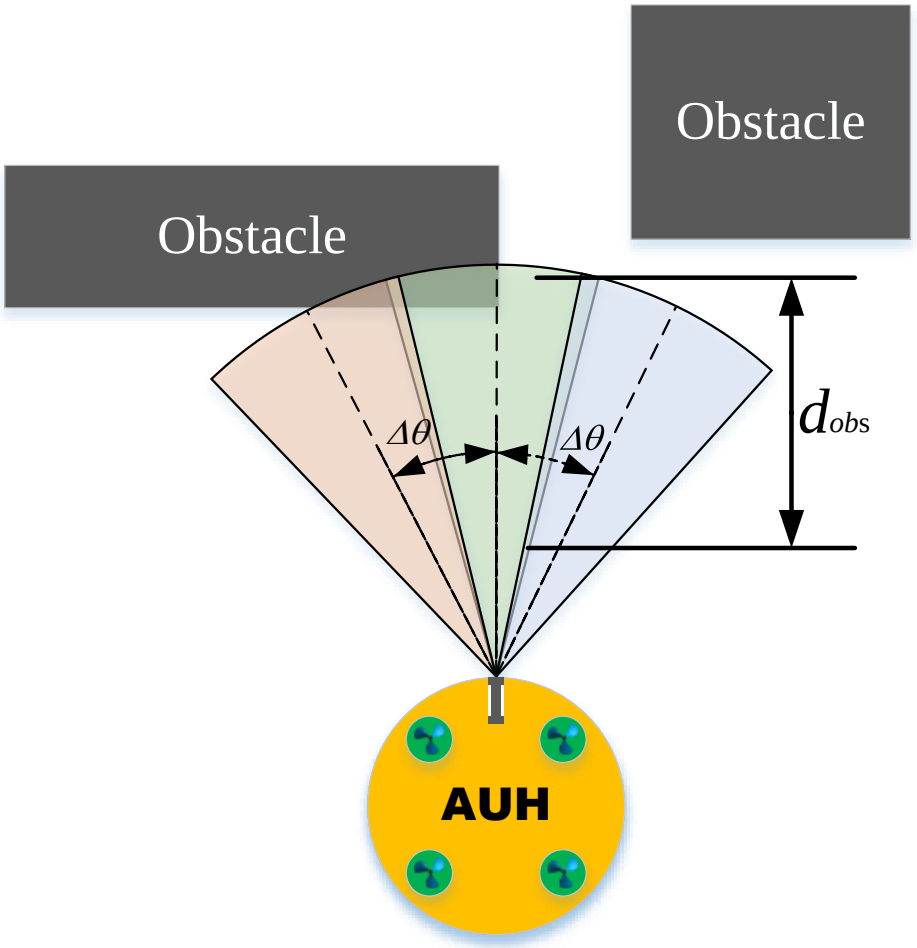

Figure 4. Obstacle range measurement strategy for AUH at a fixed position in different directions with a single-beam echo sounder.

As shown in Figure 4, taking advantage of AUH's horizontal maneuverability, it turns at different directions in an angle step of $\Delta\theta$. The distance information can be obtained in each direction with a single beam echo sounder. Assembling these distance data, obstacle information against AUH's current position is perceived, which is similar to the function of a multi-beam sonar.

These distance data are transferred to the VFH+ algorithm to determine the desired direction. The high mobility of AUH gives it an ability of multiple ranging in one location. The overall procedure of the proposed AUH's obstacle avoidance strategy is shown in Algorithm 1.

3. Simulation, Results and Discussion

3.1. Initial BCD Path Planing

In this paper, the presupposed working area for AUH is a rectangular zone. Firstly, the whole map is rasterized to small grids and AUH moves in the map step by step (as shown in Figure 5a). According to the swath width of the sonar mounted on the AUH, its one-side covering width w is determined and the traverse span w_t is influenced by the effective swath width. For the forward-looking detection sonar adopted in this case, the overlapping rate η is set to 20%; thus, $w_t = 2(1-\eta)w$. Based on BCD, with the traverse width w_t, the offline planned path for AUH is shown in Figure 5b. In Figure 5b, the green area is covered by AUH's larboard side and the peachpuff area is covered by its starboard side.

Algorithm 1: The implementation of AUH's obstacle avoidance strategy

input : AUH's starting position **A** and destination **B**;
AUH's geometric parameter r_r; Sensor's detection range; AUH's turning/danger distance d_s; Obstacle's boundary; AUH's heading θ
output: AUH's trajectory from **A** to **B**

Rasterized map;
Determine AUH's starting position and destination;
while $P_A \neq P_B$ **do**
  Move forward;
  Update P_A;
  Calculate intersection point P_S;
  $P_I \leftarrow$ *CalEndPoint*(P_A, θ);
  $P_S \leftarrow$ *CalIntersectionPoint*(P_AP_I, P_1P_2) $(P_1P_2 \in \mathbf{P})$;
  if *Detect obstacle* **then**
    $P_I \leftarrow$ *CalEndPoint*(P_A, θ);
    $P_S \leftarrow$ *CalIntersectionPoint*(P_AP_I, P_1P_2) $(P_1P_2 \in \mathbf{P})$;
    if $P_AP_S < P_1P_2$ **then**
      for $i \leftarrow 2$ **to** n **do**
        AUH's heading turns $\Delta\theta$;
        $\theta_i \leftarrow \theta + \Delta\theta$;
        $P_I^i \leftarrow$ CalEndPoint(P_A, θ_i);
        for $j \leftarrow 1$ **to** m **do**
          $P_S^{i,j} \leftarrow$ CalIntersectionPoint$(P_AP_I^i, P_1^jP_2^j)$;
          $d_{i,j} \leftarrow$ CalDistance$(P_A, P_S^{i,j})$;
        end
        $d_i = \min \mathbf{d}_j$;
      end
    end
    $P_I \leftarrow$ *CalEndPoint*(P_A, θ);
    $P_S \leftarrow$ *CalIntersectionPoint*(P_AP_I, P_1P_2) $(P_1P_2 \in \mathbf{P})$;
    if $P_AP_S < P_1P_2$ **then**
      for $i \leftarrow 2$ **to** n **do**
        AUH's heading turns $\Delta\theta$;
        $\theta_i \leftarrow \theta + \Delta\theta$;
        $P_I^i \leftarrow$ CalEndPoint(P_A, θ_i);
        for $j \leftarrow 1$ **to** m **do**
          $P_S^{i,j} \leftarrow$ CalIntersectionPoint$(P_AP_I^i, P_1^jP_2^j)$;
          $d_{i,j} \leftarrow$ CalDistance$(P_A, P_S^{i,j})$;
        end
        $d_i = \min \mathbf{d}_j$;
      end
    end
    return d ;
    for $i \leftarrow 2$ **to** n **do**
      Evaluate the obstacle range series **d** *over n directions*;
    end
    Plot the primary polar histogram over n direction at current position P_A;
    Build the binary polar histogram with two thresholds τ_{high} and τ_{low};
    Build the masked polar histogram;
    Determine the desired heading direction $\theta_{desired}$ with a cost function;
  else
    $\theta_{desired}$ keeps;
  end
  Update AUH's velocity and position;
end

AUH's online complete coverage path planning is based on the initial BCD path, and it moves forward along the initial path by going through key waypoints point-by-point. When an obstacle is encountered, the path is blocked, which means it cannot head to the next waypoint directly from its current position. Thus, it turns into a local point-to-point path planning problem for the CCPP. Once AUH circumvents obstacles and reaches the target waypoint, it can continue to move along the initial path. This procedure repeats until the whole working area is covered.

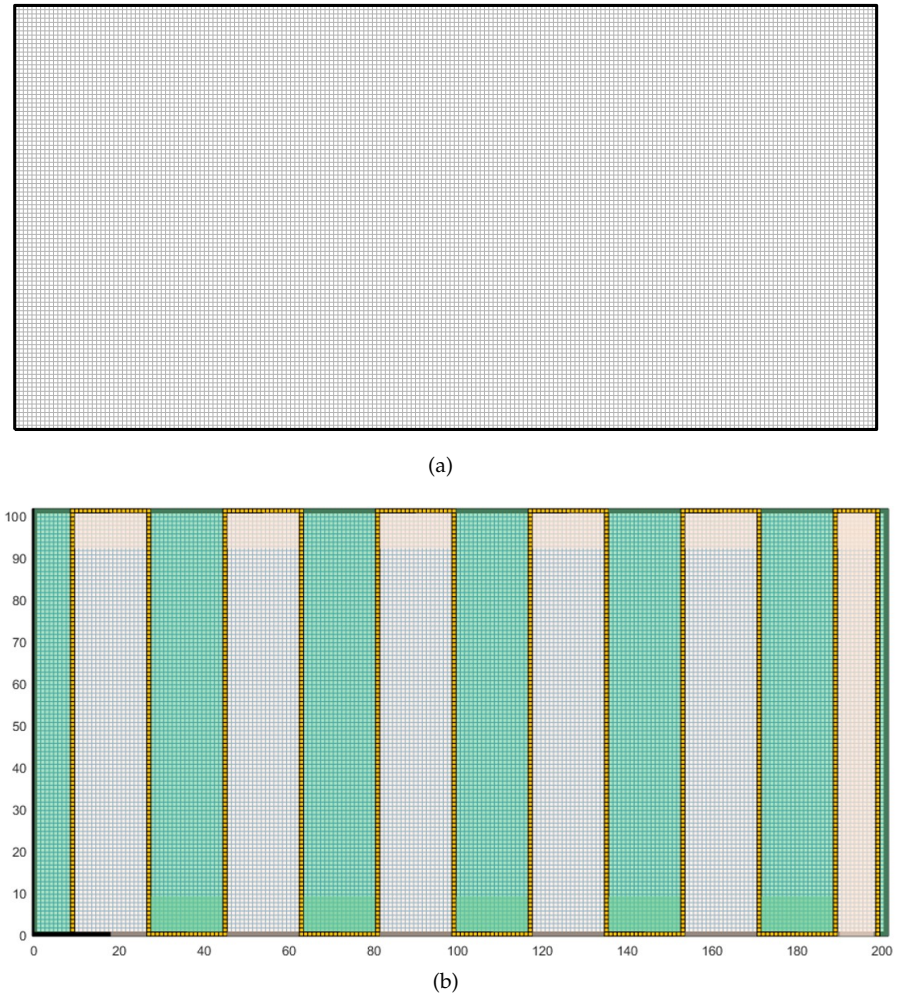

Figure 5. Initial BCD path for the complete coverage path planning. (**a**) The proposed working area with rasterized map; (**b**) Initial boustrophedon motion path.

3.2. Point-to-Point Path Planning

The point-to-point path planning consists of an offline initial way-points assignment and an online sensor-based obstacle avoidance strategy. For the preliminary way-points assignment, AUH assigns a series of way-points along the straight line between the starting position and the end position. For the obstacle avoidance function, AUH gets around sensed obstacles according to the previous mentioned strategy, that is combining multiple obstacle detection with the VFH+ algorithm. In order to explain and verify AUH's obstacle avoidance strategy in detail, a specialized point-to-point path planning problem is stated here (Figure 6) and the path planning result is discussed.

As shown in Figure 6, the initial BM designed path is blocked by an obstacle, and AUH is not available to move directly to the target waypoint from the current start position. During AUH's sailing, once the obstacle is detected by its single-beam range sensor (echo

sounder), it enters the obstacle avoidance procedure: the multiple distance measurement and heading determination at its current position.

For the simulation cases in this paper, the basic parameters related to the obstacle avoidance algorithm, such as AUH's diameter, the sailing velocity, the sensor's detection range and so on, are listed in Table 1.

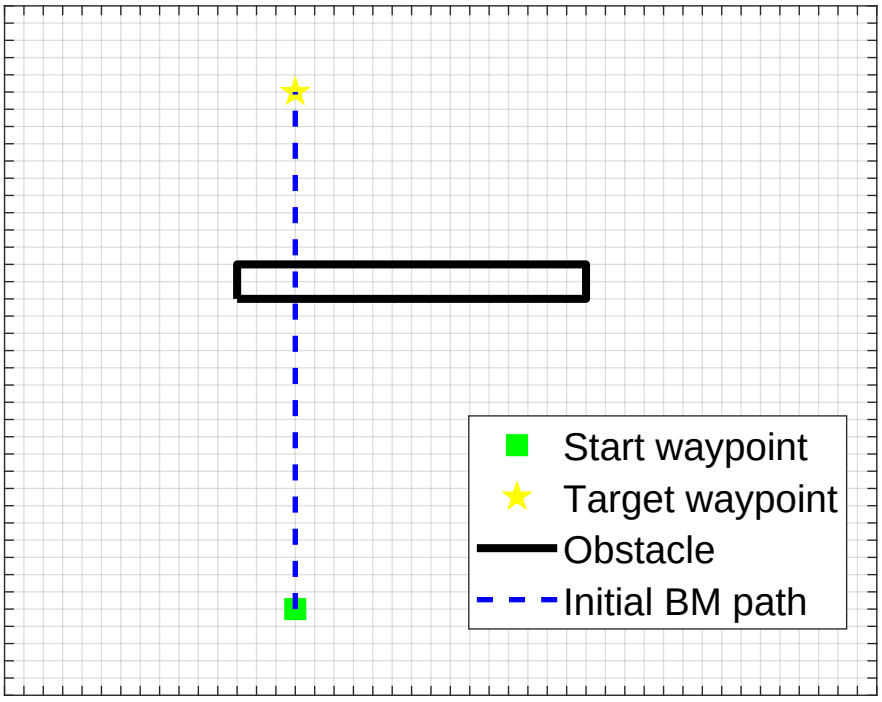

Figure 6. The statement of point-to-point path problem.

Table 1. Basic parameters related to AUH's obstacle avoidance behavior.

Parameter	Value
Diameter	2 m
Velocity	0.8 m/s
Angle step	1°
Detection range	15 m
Danger range	5 m
Detection number	15

During the simulation process, the obstacle information is unknown to AUH's decision controller, and its range to the obstacle is obtained through continuous intersection computation with the obstacles' boundaries. The entire distance measurement procedure is given in Figure 7.

It can be noted in Figure 7 that, at the first four steps, AUH's echo sounder does not detect any obstacle, so it moves forward along the initial BM path. From step 5 to step 13, AUH detects the obstacle continuously, while it continues to move forward, which means the obstacle is located in AUH's detect range, but out of the danger range, and the obstacle avoidance procedure has not been triggered. In Figure 8a, no polar histogram is plotted, which means the VFH+ algorithm is not running. During this course, multiple range measurements are carried out to gather obstacle information for the possible following decision. From step 14 onward, the obstacle approaches AUH's danger range, and the obstacle range measurement continues. Meanwhile, the obstacle range information is transferred to the VFH+ algorithm to determine the desired heading direction to bypass the detected obstacle. At this step, AUH detects the obstacle both at its larboard and starboard sides, and it can be

found in Figure 8b that block openings exist around $[0°, 80°] \cup [330°, 360°]$. Based on the obstacle information obtained at its present position, the VFH+ algorithm decides to turn left and the desired angle is 267.5°, as shown in Figure 9. From step 14 to step 19, AUH keeps moving forward and to the left. During this process, the obstacle strength slowly weakens to AUH's larboard side, as shown in Figure 8c. At step 21, the obstacle strength disappears at its left (Figure 8d). Then AUH starts moving to the target waypoint and the obstacle turns to AUH's starboard rear until it moves to AUH's right astern, as shown in Figure 8e,f. Meanwhile, AUH realizes local obstacle avoidance and slowly moves right to the target waypoint.

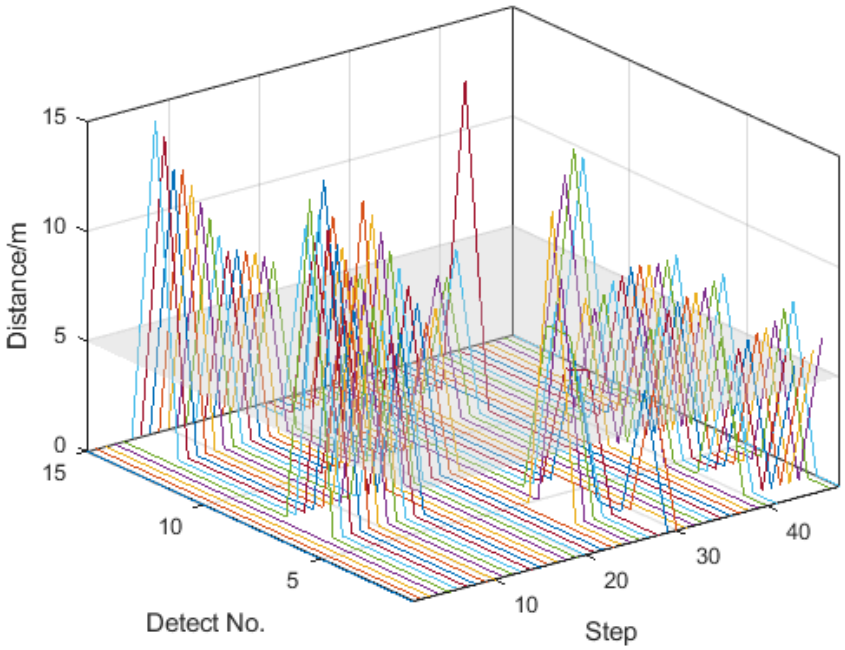

Figure 7. The distance measurement procedure during the entire local point-to-point obstacle avoidance problem. (The gray plane represents the safety distance and the color of the lines changes to indicate different steps).

The desired heading angle determined by the VFH+ algorithm during this whole procedure is shown in Figure 9.

It can be observed in Figure 9 that the desired heading conforms to the polar histograms at AUH's different move steps (Figure 8). During the entire local obstacle avoidance procedure, AUH firstly turns left according to the obtained obstacle strength. When it circumvents the obstacle, its heading direction recovers to 0°/360°. Then it turns right to get close to the target waypoint. AUH's moving trajectory in this entire procedure is shown in Figure 10.

From Figure 10, it can be verified that the obstacle avoidance proposed for AUH in this paper is suitable and feasible to make a detour around the local obstacle. Thus, combining the initial BCD path planning with the local obstacle avoidance, AUH can complete an area full coverage sweep. It is worth mentioning that the obstacle information is obtained by a single-beam echo sounder during the whole procedure. Taking advantage of AUH's horizontal mobility with multiple propellers, it has the ability to turn around at its current position. Thus, multiple obstacle range information can be gathered at various directions, which makes it function like a multi-beam range detection sonar.

3.3. Area Sweeping Path Planning

AUH is designed to work in underwater environments, and generally it works meters or tens of meters off the bottom. Obstacles at this height mainly include the seabed big bumps, and the obstacle environment is relatively simple compared to that of sweeping

robots working in a room. Hence, just some simple obstacle models are set up here. Several area sweep cases are set up to simulate the AUH's complete coverage path planning process. In Figure 11a, an obstacle is placed in the target operation area. An offline path planning process is conducted to generate the initial BM path, ignoring the existence of any possible obstacle, as mentioned above. AUH progresses along the preliminary planned trajectory and detects obstacles on the voyage. Once any obstacle is detected and approaches AUH's danger range, it enters the obstacle avoidance procedure autonomously. The online heading decision is made based on obtained obstacle range/position information and the VFH+ algorithm. AUH's final trajectory is simulated as shown in Figure 11b.

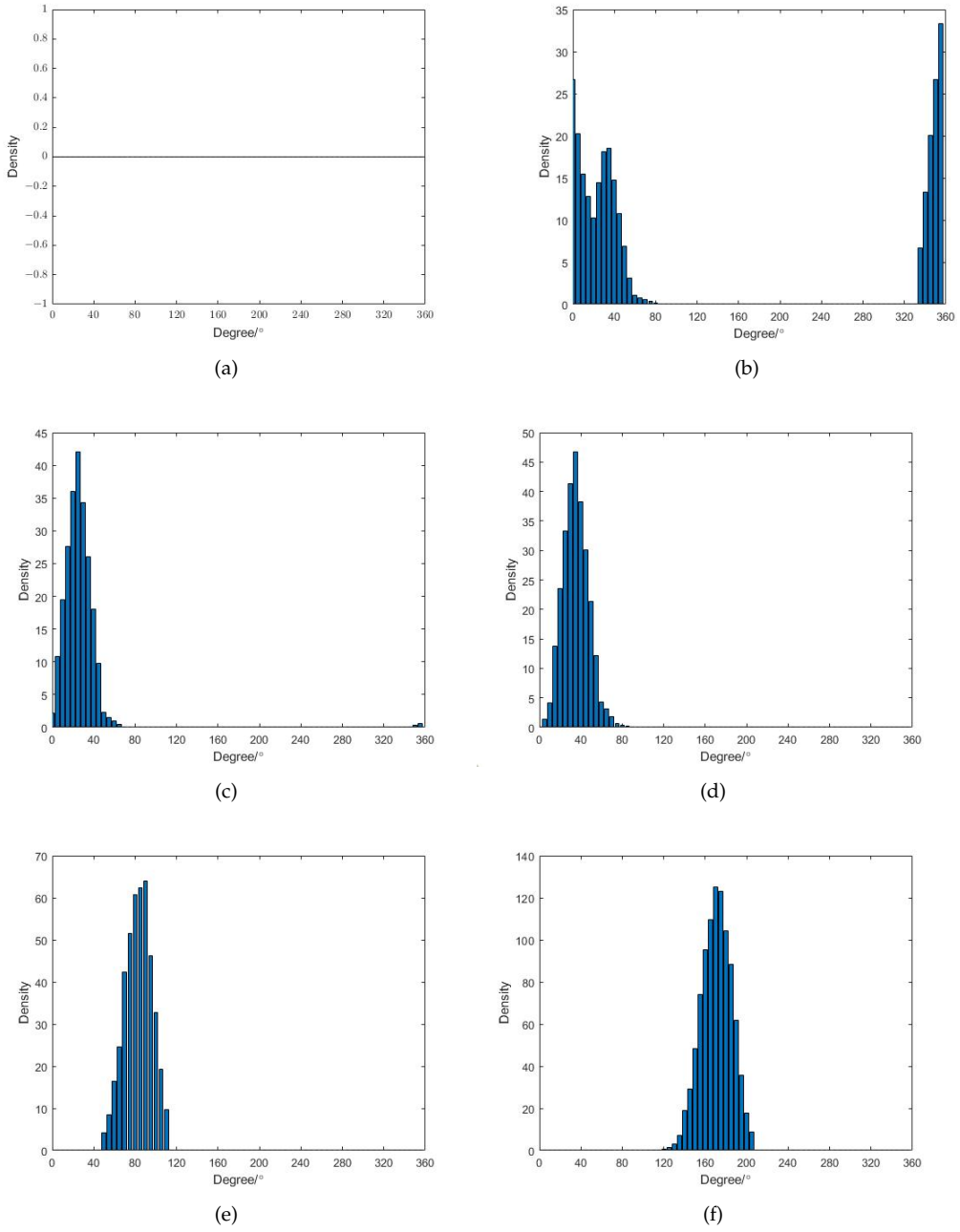

Figure 8. The polar histogram at AUH's various move steps during the obstacle avoidance procedure. (**a**) Step 13; (**b**) Step 14; (**c**) Step 19; (**d**) Step 21; (**e**) Step 30; (**f**) Step 45.

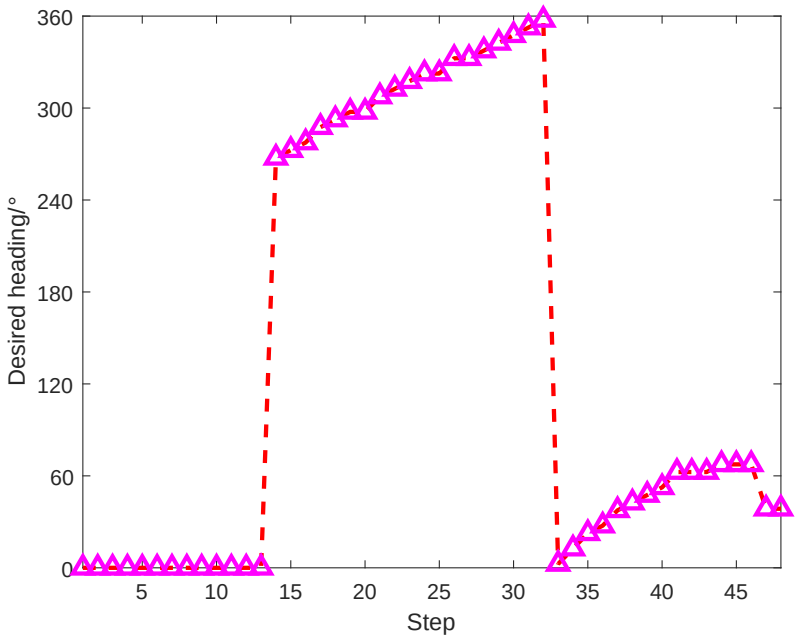

Figure 9. The desired heading angle during AUH's obstacle avoidance procedure.

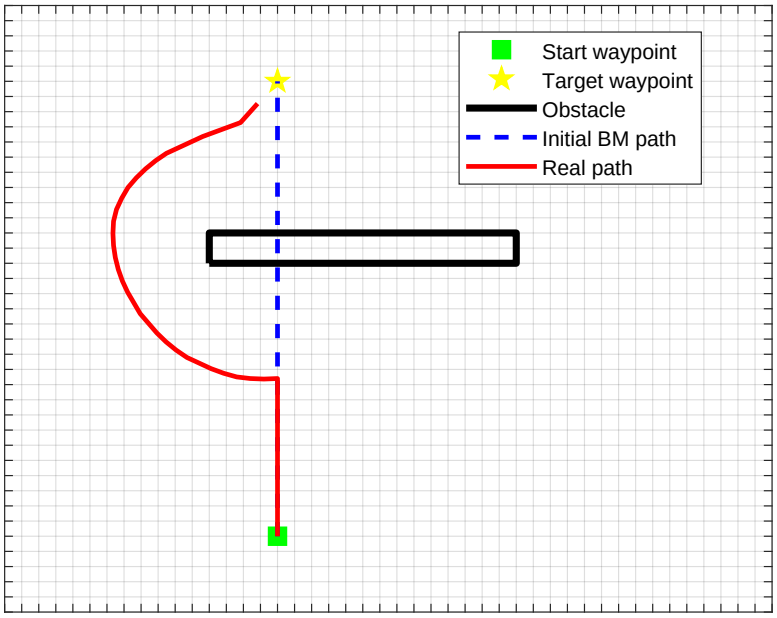

Figure 10. The planned path for the point-to-point obstacle avoidance problem with the proposed approach.

Another simulation case is established as illustrated in Figure 12a. More obstacles are placed in the sweeping area. Similar path planning process is conducted to fulfill the sweep area complete coverage.

AUH's final simulated sail track is illustrated in Figure 12b. Comparing Figure 12b with Figure 11b, it can be observed that, though the first obstacle is placed in the same position in the operation area with the same size, AUH chooses a different heading direction to bypass it. This difference is due to the existence of Obstacle 2. When AUH probes Obstacle 1, Obstacle 2 near it is also detected. The information of these two concurrent obstacles is transferred to the VFH+ algorithm, and the desired heading during this period can be seen and compared in Figure 13. According to the desired heading angle, it turns

right to circumvent Obstacle 1 in simulation case 1 (Figure 13a), while it turns right in simulation case 2 (Figure 13b). This difference demonstrates that the VFH+ algorithm can effectively avoid AUH becoming trapped in a dead-end, and the designed trajectory becomes smoother and more reliable.

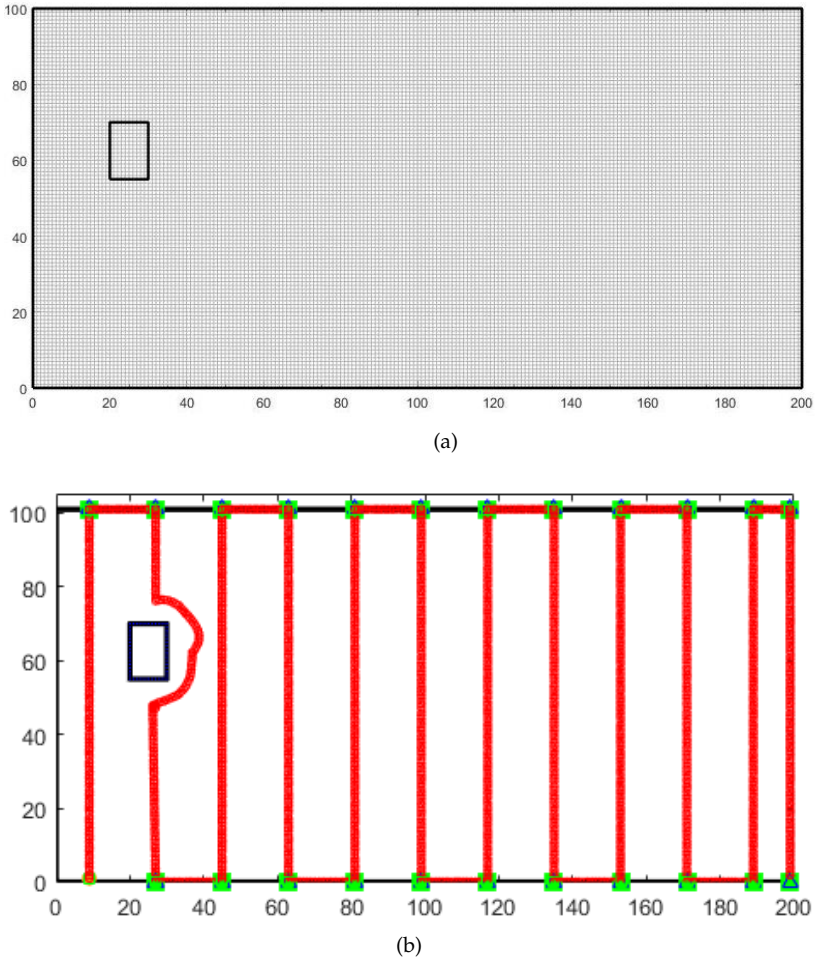

Figure 11. AUH's complete coverage area sweep simulation case 1. (**a**) Area sweep simulation setup with rasterized grids; (**b**) Area complete coverage planned path with the proposed approach. (▬: Obstacle; ▬: Real path; ■: Initial BM planned waypoint; △: Attempted waypoint.)

Figure 13 shows that, AUH can detect multiple obstacles with a single-beam echo sounder, which is essentially based on AUH's horizontal maneuverability. The disk-shape and multiple horizontal propellers layout design give AUH an advantage over the traditional torpedo-shaped AUV. This advantage makes it possible to obtain a high quantity of obstacle range information in various heading directions with a single beam range sensor; thus, the expensive multi-beam sonar is dispensed with in order to realize the same obstacle detection function. The simulation cases in Figures 11 and 12 demonstrated that the proposed online obstacle avoidance strategy is suitable for AUH with high horizontal mobility and it is feasible for AUH to fulfill a complete coverage path plan. The simulation results indicate AUH's promising application in autonomous area sweep with a low-cost single-beam range sensor.

At present, AUH's control system is running on an ARM embedded core board (Forlinx i.MX6Q, B1) and it is powered by a 1Ghz NXP quad-core ARM Cortex-A9 architecture high-performance processor. The obstacle avoidance program is intended to run on another board (NVIDIA Jetson Xavier NX, B2) and it provides 21 TOPS for accelerating computing workflow. These two boards communicate through the TCP/IP protocol. The obstacle

distance and position information is transferred from B1 to B2 in real time and the desired heading information provided by the local obstacle avoidance algorithm is transferred to B1 inversely. In addition, due to AUH's overwhelming maneuverability, it can hover at a fixed position to carry out the multiple distance measurement. Therefore, the computation load is affordable for AUH to accomplish autonomous online real-time path planning according to engineering experience, which means the CCPP strategy is reliable in practice.

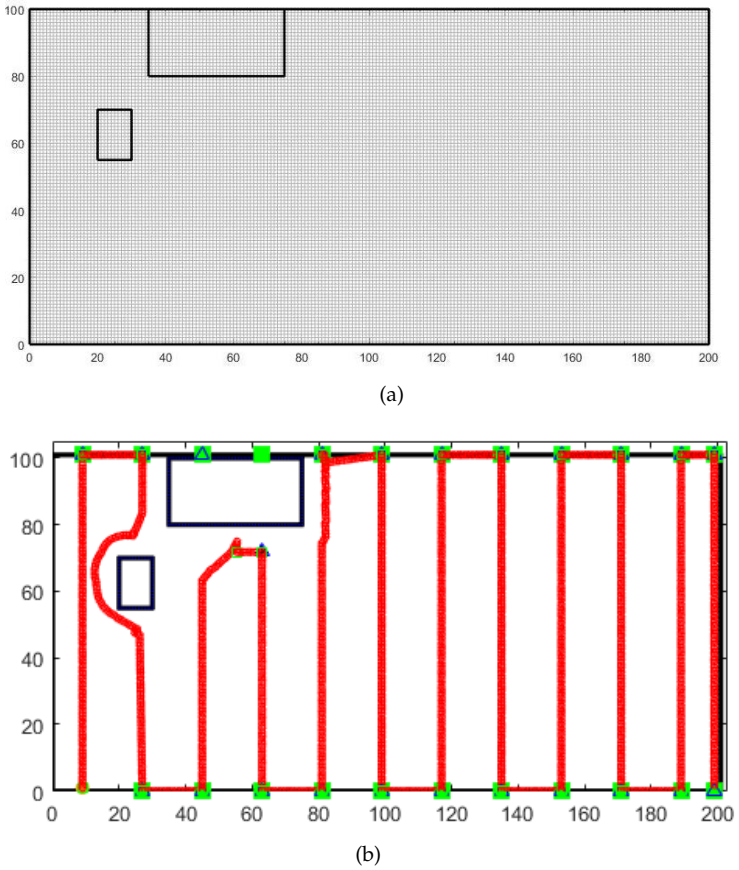

Figure 12. AUH's complete coverage area sweep simulation case 2. (**a**) Area sweep simulation setup with rasterized grids; (**b**) Area complete coverage planned path with the proposed approach. (▬: Obstacle; ▬: Real path; ■: Initial BM planned waypoint; △: Attempted waypoint.)

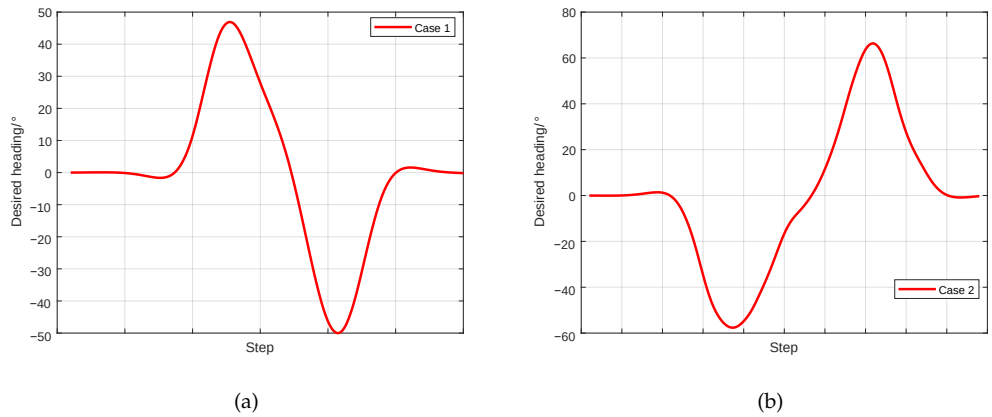

Figure 13. The variation of heading decision around obstacles in different cases. (The heading angle in $(180°, 360°]$ is mapped to $(-180°, 0°]$) for convenience. (**a**) Simulation case 1; (**b**) Simulation case 2.

4. Conclusions

The area sweep mission is a typical scenario for an AUH to operate in complex underwater environments, and complete coverage path planning is essential for AUH to accomplish this task. Based on a single-beam sonar, a CCPP approach suitable for AUH with superior horizontal mobility is proposed. The preliminary Boustrophedon Motion path planning is introduced. An obstacle detection strategy in different heading directions at a fixed position for AUH is presented, taking advantage of its maneuverability. The perceived information is then transferred to the VFH+ algorithm to make decisions on the desired heading angle. Finally, the proposed AUH's CCPP approach is implemented by combining initial path planning with the online local obstacle avoidance strategy, and its feasibility is verified through various simulation cases. The main conclusions are listed as follows:

- Taking advantage of AUH's high horizontal mobility, it can conduct obstacle range measurement in different directions at a fixed position with a single-beam echo sounder;
- Based on the multiple range measurement and the VFH+ algorithm, AUH can circumvent an obstacle effectively, which demonstrates that the obstacle avoidance strategy is feasible;
- The simulation result shows the low-cost promising collision avoidance approach for AUH with a single-beam echo sounder can fulfill a complete coverage path planning mission autonomously.

However, since AUH is designed to operate in underwater environments, encountering dead-ends is rare due to the expansive underwater world. Hence, further work is needed to apply the algorithm in practice.

- Backtracking mechanism will be developed to make the obstacle avoidance strategy more complete and AUH more intelligent;
- The transplant of proposed algorithm to AUH's controller is ongoing, which makes the algorithm move towards practical application;
- AUH's pool experiment needs to be conducted, and this application will extend to field trial and sea trial.

Author Contributions: Conceptualization, X.A. and C.M.; methodology, X.A.; software , C.M. and H.Z.; validation, X.A. and C.M.; formal analysis, X.A. and C.M.; investigation, C.M. and H.Z.; resources, X.A. and C.M.; data curation, X.A.; writing—original draft preparation, X.A.; writing—review and editing, X.A. and C.M.; visualization, X.A., C.M. and H.Z.; supervision, X.A.; project administration, X.A.; funding acquisition, C.M. All authors have read and agreed to the published version of the manuscript.

Funding: This work was supported by the National Natural Science Foundation of China (Grant No. 52001279), the Talent Introduction Research Fund of Zhejiang Ocean University (Grant No. 11105092921), the General Scientific Research Project of Zhejiang Education Department (Grant No. Y202353953) and the Zhejiang Provincial Postdoctoral Science Foundation (Grant No. ZJ2020137).

Institutional Review Board Statement: Not applicable.

Informed Consent Statement: Not applicable.

Data Availability Statement: The data presented in this study are available on request from the corresponding author. The data are not publicly available due to privacy restrictions.

Conflicts of Interest: The authors declare no conflict of interest.

Abbreviations

The following abbreviations are used in this manuscript:

AUV	Autonomous Underwater Vehicle
AUH	Autonomous Underwater Helicopter
CCPP	Complete Coverage Path Planning
BM	Boustrophedon Motion
BCD	Boustrophedon Cellular Decomposition
VFH+	Vector Field Histogram+

References

1. Zhou , J.; Huang, H.; Huang, S.; Si, Y.; Shi, K.; Quan, X.; Guo, C.; Chen, C.W.; Wang, Z.; Wang, Y.; et al. AUH, a New Technology for Ocean Exploration. *Engineering* **2022**, *25*, 21–27. [CrossRef]
2. Wang, Z.; Liu, X.; Huang, H.; Chen, Y. Development of an autonomous underwater helicopter with high maneuverability. *Appl. Sci.* **2019**, *9*, 4072. [CrossRef]
3. Chen, C.W.; Jiang, Y.; Huang, H.C.; Ji, D.X.; Sun, G.Q.; Yu, Z.; Chen, Y. Computational fluid dynamics study of the motion stability of an autonomous underwater helicopter. *Ocean. Eng.* **2017**, *143*, 227–239. [CrossRef]
4. Lin, Y.; Huang, Y.; Zhu, H.; Huang, H.; Chen, Y. Simulation study on the hydrodynamic resistance and stability of a disk-shaped autonomous underwater helicopter. *Ocean. Eng.* **2021**, *219*, 108385. [CrossRef]
5. An, X.; Chen, Y.; Huang, H. Parametric design and optimization of the profile of autonomous underwater helicopter based on NURBS. *J. Mar. Sci. Eng.* **2021**, *9*, 668. [CrossRef]
6. Lin, Y.; Guo, J.; Li, H.; Wang, Z.; Chen, Y.; Huang, H. Improvement of hydrodynamic performance of the disk-shaped autonomous underwater helicopter by local shape modification. *Ocean. Eng.* **2022**, *260*, 112056. [CrossRef]
7. Li, H.; An, X.; Feng, R.; Chen, Y. Motion Control of Autonomous Underwater Helicopter Based on Linear Active Disturbance Rejection Control with Tracking Differentiator. *Appl. Sci.* **2023**, *13*, 3836. [CrossRef]
8. Hu, S.; Feng, R.; Wang, Z.; Zhu, C.; Wang, Z.; Chen, Y.; Huang, H. Control system of the autonomous underwater helicopter for pipeline inspection. *Ocean. Eng.* **2022**, *266*, 113190. [CrossRef]
9. Rooban, S.; Joshitha, C.; Eshwar, I.V.S. Surveillance and Obstacle Avoiding Autonomous Robot. In Proceedings of the 2021 Asian Conference on Innovation in Technology (ASIANCON), Pune, India, 27–29 August 2021; IEEE: Piscataway, NJ, USA; pp. 1–6.
10. Sandamurthy, K.; Ramanujam, K. A hybrid weed optimized coverage path planning technique for autonomous harvesting in cashew orchards. *Inf. Process. Agric.* **2020**, *7*, 152–164. [CrossRef]
11. Cheng, C.; Sha, Q.; He, B.; Li, G. Path planning and obstacle avoidance for AUV: A review. *Ocean. Eng.* **2021**, *235*, 109355. [CrossRef]
12. Khan, A.; Noreen, I.; Ryu, H.; Doh, N.L.; Habib, Z. Online complete coverage path planning using two-way proximity search. *Intell. Serv. Robot.* **2017**, *10*, 229–240. [CrossRef]
13. Debnath, S.K.; Omar, R.; Bagchi, S.; Sabudin, E.N.; Shee Kandar, M.H.A.; Foysol, K.; Chakraborty, T.K. Different cell decomposition path planning methods for unmanned air vehicles—A review. In Proceedings of the 11th National Technical Seminar on Unmanned System Technology 2019: NUSYS'19, Kuantan, Malaysia, 2–3 December 2019; Springer: Singapore, 2021; pp. 99–111.
14. Karapetyan, N.; Moulton, J.; Lewis, J.S.; Li, A.Q.; O'Kane, J.M.; Rekleitis, I. Multi-robot dubins coverage with autonomous surface vehicles. In Proceedings of the 2018 IEEE International Conference on Robotics and Automation (ICRA), Brisbane, QLD, Australia, 21–25 May 2018; IEEE: Piscataway, NJ, USA; pp. 2373–2379.
15. Lewis, J.S.; Edwards, W.; Benson, K.; Rekleitis, I.; O'Kane, J.M. Semi-boustrophedon coverage with a dubins vehicle. In Proceedings of the 2017 IEEE/RSJ International Conference on Intelligent Robots and Systems (IROS), Vancouver, BC, Canada, 24–28 September 2017; pp. 5630–5637. [CrossRef]
16. Acar, E.U.; Choset, H.; Rizzi, A.A.; Atkar, P.N.; Hull, D. Morse decompositions for coverage tasks. *Int. J. Robot. Res.* **2002**, *21*, 331–344. [CrossRef]
17. Huang, W. Optimal line-sweep-based decompositions for coverage algorithms. In Proceedings of the 2001 ICRA. IEEE International Conference on Robotics and Automation (Cat. No.01CH37164), Seoul, Republic of Korea, 21–26 May 2001; Volume 1, pp. 27–32. [CrossRef]
18. Fu, X.; Zhi, C.; Wu, D. Obstacle avoidance and collision avoidance of UAV swarm based on improved VFH algorithm and information sharing strategy. *Comput. Ind. Eng.* **2023**, *186*, 109761. [CrossRef]
19. Pappas, P.; Chiou, M.; Epsimos, G.T.; Nikolaou, G.; Stolkin, R. Vfh+ based shared control for remotely operated mobile robots. In Proceedings of the 2020 IEEE International Symposium on Safety, Security, and Rescue Robotics (SSRR), Abu Dhabi, United Arab Emirates, 4–6 November 2020; IEEE: Piscataway, NJ, USA; pp. 366–373.
20. Viet, H.H.; Dang, V.H.; Laskar, M.N.U.; Chung, T.C. BA*: An online complete coverage algorithm for cleaning robots. *Appl. Intell.* **2013**, *39*, 217–235. [CrossRef]

21. Lakshmanan, A.K.; Mohan, R.E.; Ramalingam, B.; Le, A.V.; Veerajagadeshwar, P.; Tiwari, K.; Ilyas, M. Complete coverage path planning using reinforcement learning for tetromino based cleaning and maintenance robot. *Autom. Constr.* **2020**, *112*, 103078. [CrossRef]
22. Wenzel, P.; Schön, T.; Leal-Taixé, L.; Cremers, D. Vision-based mobile robotics obstacle avoidance with deep reinforcement learning. In Proceedings of the 2021 IEEE International Conference on Robotics and Automation (ICRA), Xi'an, China, 30 May–5 June 2021; IEEE: Piscataway, NJ, USA; pp. 14360–14366.
23. Gonzalez-Garcia, A.; Collado-Gonzalez, I.; Cuan-Urquizo, R.; Sotelo, C.; Sotelo, D.; Castañeda, H. Path-following and LiDAR-based obstacle avoidance via NMPC for an autonomous surface vehicle. *Ocean. Eng.* **2022**, *266*, 112900. [CrossRef]
24. Li, C.; Guo, S.; Guo, J. Study on obstacle avoidance strategy using multiple ultrasonic sensors for spherical underwater robots. *IEEE Sens. J.* **2022**, *22*, 24458–24470. [CrossRef]
25. Huang, X.; Dong, X.; Ma, J.; Liu, K.; Ahmed, S.; Lin, J.; Qiu, B. The improved A* Obstacle avoidance algorithm for the plant protection UAV with millimeter wave radar and monocular camera data fusion. *Remote Sens.* **2021**, *13*, 3364. [CrossRef]
26. Morency, C.; Stilwell, D.J. Evaluating the Benefit of Using Multiple Low-Cost Forward-Looking Sonar Beams for Collision Avoidance in Small AUVs. In Proceedings of the 2022 IEEE/RSJ International Conference on Intelligent Robots and Systems (IROS), Kyoto, Japan, 23–27 October 2022; IEEE: Piscataway, NJ, USA; pp. 8423–8429.
27. Ulrich, I.; Borenstein, J. VFH+: Reliable obstacle avoidance for fast mobile robots. In Proceedings of the1998 IEEE International Conference on Robotics and Automation (Cat. No. 98CH36146), Leuven, Belgium, 20 May 1998; IEEE: Piscataway, NJ, USA; Volume 2, pp. 1572–1577.